Synthesis of silicone oil based magnetorhelogical fluid and performance analysis in a landing gear using bat-based gradient boost mechanism

Selvaraj Suseela Stalin[1], Marimuthu Uthayakumar[2], P. Balamurugan[1],
M. Pethuraj[3], Jerzy A. Sładek[4], Magdalena Niemczewska-Wójcik[4*]

1 Faculty of Mechanical Engineering, Kalasalingam Academy of Research and Education, 626126, Krishnankoil, India
2 Amrita Vishwa Vidyapeetham, Department of Mechanical Engineering, 690525, Amritapuri, India
3 Saveetha Institute of Medical and Technical Sciences, Department of Mechanical Engineering, Saveetha School of Engineering, Chennai, India
4 Faculty of Mechanical Engineering, Cracow University of Technology, al. Jana Pawła II 37, 31-864 Cracow, Poland
* Corresponding author's e-mail: magdalena.niemczewska-wojcik@pk.edu.pl

ABSTRACT

Aircraft landing gear is used to reduce the vibration and impact load that is transmitted from the ground to the aircraft body. This paper aims at investigating the application of the Magneto-Rehological damper in the landing gear system which provides high amplitude damping force through the variation of the external magnetic field. The control and reliability of the MR damper were numerically analyzed and experimentally tested in order to meet the aviation standards. The present research proposes a new Magneto-Rheological fluid combined with a Bat-based Gradient Boost Mechanism to manage damping parameters and current. The Magneto-Rheological fluid was developed with iron and silicon additives and was incorporated into a landing gear system in the form of an MR fluid damper designed using ANSYS. Optimum design parameters of the damper were analyzed in MATLAB with the help of Bat-based Gradient Boost Mechanism. The performance of the proposed Magneto-Rehological fluid damper was very encouraging, it produced a high damping force and low stroke rate with maximum yield stress of 160 kPa at a flux density of 1.4. The minimum stroke was 0.185 m and the energy efficiency obtained was 96.7%. Laboratory tests gave results of maximum damping force of 2.4 kN, the yield stress of 160 kPa together with the stroke of 0.185 m which is almost close to the theoretical analysis. The friction force of the damper was measured at -210 nN prior to the optimization whereas, before the optimization it was -58 nN only.

Keywords: magneto-rheological fluid damper, damping force, landing gear, current regulation, stroke and displacement.

INTRODUCTION

Nowadays, Magneto-Rheological (MR) fluid is the location of notable position based on the potential application of certain areas [1]. MR dampers are used in several application such as body armor, prosthetic legs, automobiles, home applications such as washing machines and mixer grinders to control the vibration [2]. It consists of interruption of iron particles and is there in micro size. The carrier fluid contains a micro-size range of up to 10 micrometers containing mineral oil, glycol, water, and hydrocarbon oil [3]. MR fluid is anintelligent material organization; hence it has rheological conduct [4]. While the magnetic field is applied, it will change the property of the liquid into a semi-solid state. MR fluid is the best material to develop a semi-active system and allow controllability [5]. Consequently, MR fluid is a highly controllable device in a fluid state. Whether any magnetic fields enter the MR fluid will change into a semi-solid state [6]. So, MR fluid is incorporated and implemented with a semi-active damper [7]. MR dampers are the semi-active control scheme, and they are generally used for several applications like tremor attenuation, automotive suspension,

prosthetic limb, landing gear, and seismic structural controllers [8]. While the MR damper is filled with MR fluid, it has gained interest because of its low power depletion, response time, and controllability. The damper is a hydraulic or mechanical device that absorbs vehicle shock impulse and reduces the vehicle suspension [9]. The dampers contained magnetic effect is transmitted to the dumpling through eddy current, and it will transfer mechanical energy into the current. Furthermore, MR dampers have the reliability to provide better performance in minimizing production price and no need for maintenance [10]. Additionally, the main disadvantage of the MR fluid is a particle of iron sets because of incompatibility of density among heavy magnetizable elements and base fluid. Thus the particle is undergoing the setting of MR fluid and ensures constancy reduction [11]. Due to the effect of Brownian motion, the acknowledgment of magnetic elements contained in the oil is hard sufficient [12]. Subsequently, a lot of research is developed to advance MR fluid's constancy, improve the steadiness of fluid, and modify the components of iron particles [13]. In addition, the high behavior of MR fluid with damper is the most challenging task, which needs lots of uncounted techniques and characteristics. With the growing interest in MR dampers, several types of research are proposed to hysteretic actions to improve the control accuracy in parameters and improve control robustness [14]. The existing techniques are MR damper-based hysteresis technique [15], adaptive control technique [16], MR suspension model for road testing [17], and load-leveling suspension mode [18]. But still has issues in control vibration and MR fluid damage because of long-term operation. So this paper developed a new framework for preventing vibration in MR damper, steadiness, and robustness control. Moreover, MATLAB and ANSYS tools are used to validate the damper performance. The damper parameters are attained from the experimental process then the parameter of the damper is given to MATLAB [19]. The hybrid optimization function has been processed to tune the parameters. Finally, stress, strain, and magnetic flux results are obtained, which is given to the ANSYS. Finally, the optimized damper is designed in an ANSYS environment, and performances are validated. Daniel Cruze *et al.* [20] proposed six MR fluids for the potential talk of several applications, and the generated fluid has the percentage of approved liquid and carbonyl Iron (CI). The effect of carried liquid is tested with the help of CI and

carrier oil. The experimental and numerical study of the soft impact is harvested in piezoelectric energy, and they are inserted as the thin layer in MR fluid. Sylvester *et al.*[21] introduced an object impact that is used for mechanical purposes such as the suppressor of the automobile. Finally, the introduced technique gained high performance in frequency amplification. Due to inelastic behavior, it will affect the overall processing time and obtain a large time delay. Asan *et al.* [22] have introduced a particle swarm technique for enhancing the detection of sample parameters. Thus the developed framework directly controls the value of fluid and reduces the error by the empirical response. An experimental outcomes are compared to the Bouc-Wen replica actions with the help of particle swarm actions. Thus the actions of the parameter are detected using genetic technique, and the experimental outcomes of developed replica attain good performance in detecting parameter. But it will affect the MR fluid because of long-term operation. Based on the electromagnet, two permanent magnets are introduced to analyze the characteristics of the MR fluid damper. Olivier and Jung [23] have proposed an MR damper to generate the magnetic field and increase different electromagnets. Additionally, developed hybrid MR is designed to analyze the values of magnetic flux. The force of damping is also selected for the objective function and identifies the optimal solution of hybrid MR. The developed replica provides a large quantity of damping force and lower electric energy consumption. But high shear rate because of overtime. Mario versatile *et al.* [24] have developed an asymmetric MR damper for using the finite element technique. A steady-state current can circulate the coil in the device, and the magnetostatic examination is stripped to the MR fluid. The device is heating during processing time, and an examination of the thermostatic is carried out with the help of finite elements. The proposed replica provides information about the temperature of MR fluid and the magnetic particle. But they execute a long time to computation, and the energy consumption is high. Thiyagu et al. studied the Nano-textured carbide tool insert with Magnetorheological Graphene Coatings for turning of DSS S31803/2205. By employing the Box–Behnken design, the results have shown high-performance graphene-coated inserts with 0.298 mm flank wear after 21 passes, uniform tem- perature of 202 °C at 55 m/min, and exceptionally better wear resistance from cementite as well as ultrafine grain boundaries [25].

The presented in this work research is arranged as follows, syntesis of MR fluid by varying the composition of Silicone Oil and CI powder, modelling and performance analysis of MR dampers used in landing gear with and without BGBM control algorithm using MATLAB and Ansys environment and Experimental study on dampers with MR fluid employed followed by conclusion.

MATERIALS AND METHODS

Synthesis of MR fluid

The MR fluid is a smart fluid whose behaviour can be controlled by applying a magnetic field to it, the carrier liquid is a multiphase noncolloidal dispersion of magnetisable particles in a nonmagnetic fluid. The dispersed particles are typically micron in size, and the liquid phase can consist of a stable and inert fluid-like silicone oil, hydrocarbon oil, mineral oil, or paraffin oil. Due to their higher limit of magnetic saturation, high purity, and distinctive particle form, magnetic iron particles obtained from thermal breakdown of iron pentacarbonyl are chosen in this circumstance. In this current research the four MR fluid samples are prepared by varying the weight percentage of silicon oil, lithium stearate, Tergitol NP10, and carbonyl iron. Table 1 shows the various composition of the MR Fluids. The MR fluids properties are density are $3 \times 10^3 - 4 \times 10^3$ kg/m³, maximum energy density 10^5 J/m³, flow stability ratio $10^{-10} - 10^{-11}$ s/Pa, operation temperature range 40 °C and coefficient of thermal expansion 0.66 e^{-3}(1/°C).

Modelling of structure of MR damper landing gear

The damping force in MR damper landing gear can be modified based on the magnetic field intensity of the passage where MR fluid flows with the damper's motion. The structure of the MR damper landing gear is identical to that of a traditional passive oleo-pneumatic landing gear system, with the exception of an annular cross-sectional flow route in the piston to maximise the characteristics of the MR fluids. In this research work, a normal MR damper was modelled and performance was studied using MATLAB and Ansys software. To improve the performance a novel BGBM was designed to control the electrical application, i.e. the current signal in the MR dampers in Landing gear. Finally, the key metrics are calculated and compared with other models of damping force, F-value, flux density, stress, and error.

According to the material properties of the damper, for piston rod is a non-magnetic hardened chromium plated stainless steel is used, for cylinder and piston head carbon steel are used which has a good magnetic conductivity and structural strength. The excitation coil part is wound with enameled copper wire evenly with multiple turns. Bobbins are made up of nylon materials. The design parameters of the MR damper are shown in Table 2. The designed MR fluid damper is a semi-active gadget that has afforded a wide measure of the controllable damping force functioning under the valve mode. Moreover, the damping force was varied based on the properties, size, and flow measure of MR fluid in the damper.

Initially, the MR damper is designed with before optimization values such as piston radius, piston height, flow way gap, coil, offset, height and width. Consequently, the performance was noted and the actual design values were optimized using BGBM. Next the perfroamnce studies were done on the remodelelled damper. Figure 1 shows the BGBM based MR damper modelled using Ansys environment.

The design parameter of damper's before and after optimization is detailed in Table 2. Here, represents radius, has denoted gaps, coil design is exposed as, is the coil height and is the coil width. To maximize the damping performance, the damper controller is analyzed and regulated using the BGBM model, based upon the optimized value again, the damper was remodelled.

Table 1. Composition of MR fluids

Constituents	Sample 1 [g]	Sample 2 [g]	Sample 3 [g]	Sample 4 [g]
Silicone oil	55.59	53.28	57.621	59.341
CI powder	19.236	21.896	38.36	51.36
Lithium stearate	7.476	11.806	18.216	21.216
Tergitol NP10	1.512	2.016	2.782	1.928

Table 2. Design parameters of damper (before and after optimization)

Design parameter	Unit	Parametric values	
		Before optimization	After optimization
Outer diameter of the cylinder	mm	75	75
Cylinder wall thickness	mm	4	4
Length of the cylinder	mm	166	166
Stroke length	mm	80	80
Diameter of the piston	mm	66	67
Length of the piston	mm	52	50
Diameter of the piston pin	mm	20	20
Damping gap thickness	mm	1.5	1.2
Injection hole diameter	mm	4	4
Depth of the bobbin	mm	35	35
Diameter of the bobbin	mm	10.5	8.5
Number of bobbin	nos	2	2
Turns of coil	nos	1160	1160
Copper wire	swg	26	26
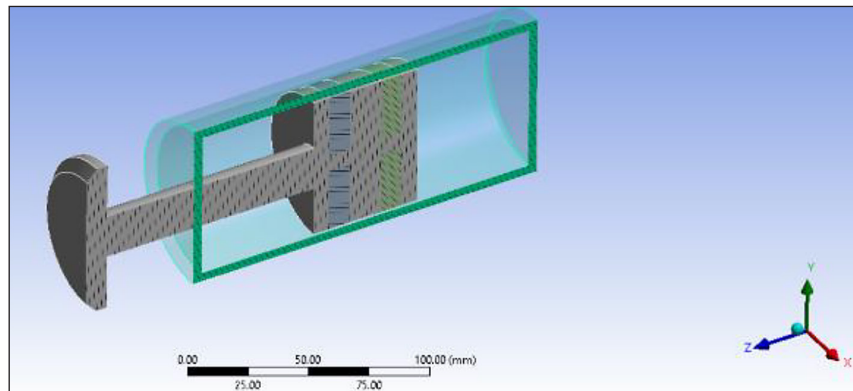
Figure 1. Internal design of proposed MR damper with BGBM

Moreover, the material was designed with the B and H arc values, which magnitude of field intensity, and MF density.

The projected damper function was designed with the following mathematical functions; hence, the damping function is detailed as Equation 1

$$target\,d_f = \frac{\int_0^{p_{max}} d_f\,ds}{0.9\,p_{max}} \quad (1)$$

where: the target damping force is denoted as $target_v$, and the high damping force is determined as p_{max}. Based on the vibrant energy, the force of damping differed; also that is based on aircraft speed and mass.

$$ic = \begin{cases} 0 & target_V < V \\ target_V - V & target_V \geq V \end{cases} \quad (2)$$

Now the input of the control module is defined using Equation 2, here V is the damping force. For each landing condition, the target value differed.

In the present research, the intelligent controller is made by neural model and optimization concept. Here, the trained database is, b_m, b_n and c_m, also the V parameter is exposed as $V = (v_1...v_n)$. Then the loss parameter of the BGBM was measured in Equation 3.

$$f(V) = arg\,min \quad V\,[V_r\,(\psi\,[r,f(V)]|V| \quad (3)$$

Here, r denotes response variable, the traceable parameter to track the mass of aircraft is determined as $f(Bf, \theta)$. Now the mass estimating function of system with the support of the bat fitness is valued using Equation 4

$$f(Bf) = f(Bf, \theta) \quad (4)$$

Therefore, the working of the damping force is scale in Equation 5, here, is the random target force.

$$V_i = V_{min} + (V_{max} - V_{min})\Omega \qquad (5)$$

The designed damper function is controlled by the pseudocode exposed in Algorithm 1. The input parameters for BGBM algorithm are Magnetic Field Intensity 1.0 T to 1.5, MR Fluid Yield Stress 80 kPa to 170 kPa, Frictional Loss -250 nN to -50 Nn, and Energy Efficiency 90 to 98%. Also, this controlling function has developed in the MATLAB R2020 band executed in the windows 10 environment. The workflow of the proposed procedure is detailed in Figure 2(a), here, MR fluid properties are taken in the form MF density and field intensity as shown in Figure 2(b). Moreover, the gathered MR fluid parameters are used as the damper design coefficients.

Experimental analysis

The MR damper is tested using the suspension test apparatus. The test rig generates sinusoidal excitation at various velocities and the readings are taken by varying the current supplied to the electromagnet. The magnitude of excitation was provided by the scotch yoke mechanism, which allows the shaft offset distance to be changed. The scotch

Algorithm 1

```
Start
{
        Initializing the MR damper design parameters
        {
```
$$Int \; r, \; V \; ;$$
$$f(V) \rightarrow r(V)$$
```
            // the damping force is differed based on the response variable.
        }
        Damping force control
        {
```
$$Initialize \rightarrow bat \; fitness$$
$$f(B) \rightarrow f(V)$$

// here $f(B)$ is the bat fitness

$$E = b_m, b_n, c_m, c_n$$

// Here, b_m, b_n, c_m, c_n are the aircraft parameters and E is the estimating variable

$$GW = t(b_m, b_n, c_m, c_n)$$

//where, GW is the layer weighting variable and t is the training set parameter

$$set \rightarrow \min(V) \; \& \; \max(V)$$

// fixing minimum and maximum damping force

$$Re \; gulate(V) = E(aircraft \quad mass)$$

```
            //the force of damper was based on aircraft mass
            Return E(optimum value)
        }
}
Stop
```

yoke was set to an offset value of 0.8, 1, 1.5, and 2 mm for testing reasons. For suspension mounting, two supports that can move vertically up and down were used. The lower support is linked to the scotch yoke mechanism, which generates variable sinusoidal excitation, whereas the top support height can be varied according to the length of the suspension and is fixed using locking plates. The coupling connects the scotch yoke mechanism to the DC motor. A dimmer stat was used to alter the voltage supply to the DC motor in order to vary the speed of the electric motor. The readings are taken by varying the current supplied to the electromagnet. Figure 3 depicts the suspension test rig configuration.

RESULT AND DISCUSSION

Simulation analysis

In this research damper design is constructed in the ANSYS simulation tool, and the control function to reduce the damping force is executed in the MATLAB platform. Once the damper is developed in the ANSYS framework, the values of the parameters that have to be optimized are identified. The damper is designed mathematically in the MATLAB tool, and the control algorithms are developed and consequently, the values taken from the ANSYS

are considered as the input of the control algorithm then finally, optimized variables are obtained. Subsequently, based on the optimized value, the damper is regulated then the damper's performance is noted.

Damper has been generated using MR fluid yield stress, and then the landing gear motion is detailed in Equation 6 and 7. Where Body mass in the aircraft is denoted as b_m, tire mass is defined as b_n, c_m denotes body displacements and represented tire displacement.

$$b_m c_m = -[V_{air} + V_{vis} + V_{mr}] - b_m g \qquad (6)$$

$$b_n c_n = -[V_{air} + V_{vis} + V_{mr}] - b_n g \qquad (7)$$

In this case analysis, the parameters are taken in the way of = 700 kg,=19 kg. Also the stiffness of the tire is 411,000 N/m, and the parameter damping force is denoted as .The constraints of this proposed design are exposed as follows; the peformance rate of the landing gear is in the range of 70 to 85%. Moreover, the 1mm inner gap size is commonly utilized to minimize the phenomenon block. The MR fluid damper in the experimental setup is described in detail in Figure 3. The designed BGBM damper has the capability to handle a wide range of stress. The minimum damping force has been attained while the 50 mm core length. Eqn measured
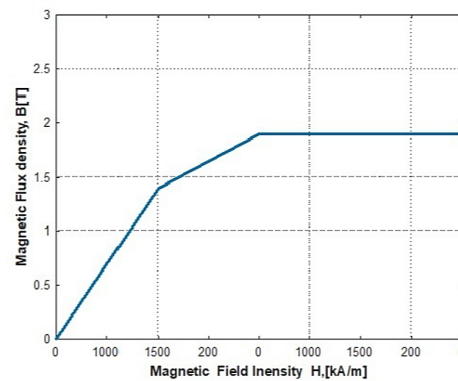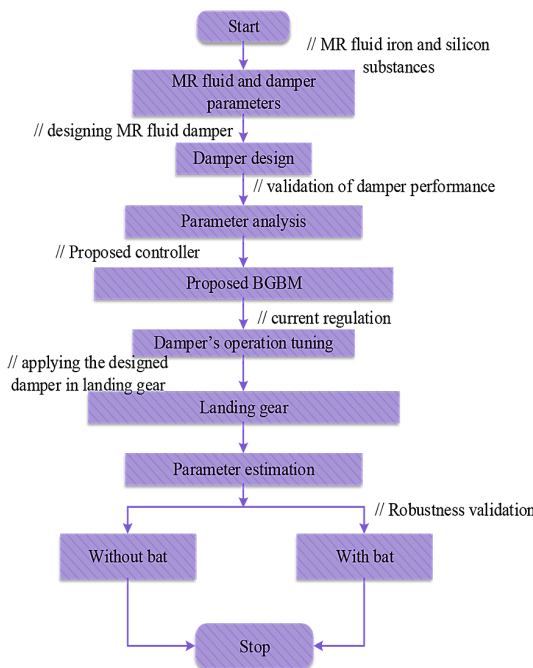

Figure 2. Process of the BGBM-MR fluid damper (a) and B-H curve of the designed damper (b)
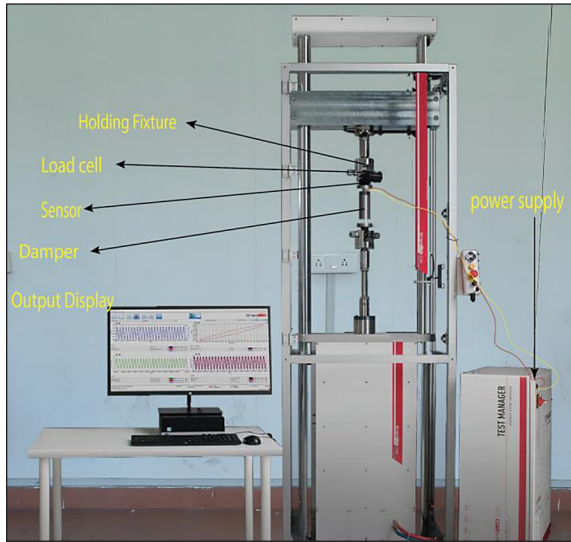
Figure 3. Experimental setup suspension test rig attached with of MR damper

$$\eta = \frac{\int_0^{p_{final}} V \, ds}{p_{max} V_{max}} = \frac{\int_0^{p_{max}} V \, ds}{p_{max} V_{max}} + \frac{\int_{p_{max}}^{p_{final}} V \, ds}{p_{max} V_{max}} \qquad (9)$$

The amount of magnetic field (MF) lines interrupted through the given closed area is termed MF. Moreover, the area is in any orientation or size, which respects the MF direction. Also, the MF is represented as , now, the FD was valued by Equation 10. The angle at which the MF line passes through in between the allocated area is defined as . Here, the MF is represented as , and the surface is denoted as .

$$\phi_B = B.S = BS \cos \Theta \qquad (10)$$

where: the flux density of the designed damper is analyzed by different gaps that are 0.8, 1, 1.5 and 2. In that, for 0.8 and 1 annular gap MF density, similar values are reported. This shows the stability range of the damping force. In addition, the damper's movement is based on the MF values. Due to the magnetic flux, similar repression bulk materials are removed; it maximizes the MR damper's static properties. The results of MF density and Current in damples are reported in Table 3. Figure 4 displays the 3D graph of the output values reported after BGBM process i.e. 160 kPa for 1.4 MF densities.

the landing gear efficiency score based on the energy-absorbing capacity. (9), and the landing gear is denoted as, and the tuning function is processed using Equation 8.

$$\alpha = \frac{\int V_{strut} \, ds}{V_{strut-max} \cdot P_{max}} \qquad (8)$$

To value the successive measurements of the Landing gear, the BGBM controller is utilized. Then the utilized novel BGBM controller is valued with other old controllers.

When thehas touched the land, then the specific system's initial potential and kinetic energywas dissipated and absorbed with the damper's back-and-forth motion. The process of the dampers was valued by taking the integral of V. In addition, after the construction of system, the damping force was stabilized; after that, potential and kinetic energy were validated. The constant potential and kinetic energy are initially trained to the framework. On the other hand, the proficiency score of the damper design is valued by evaluating the measure of stroke and Vmax force.

Experimental analysis

As the current increases, the sample with higher particle composition shows the greatest increase in damping force developed. It is obtained that sample 4 is the ideal choice for MR fluid for the viscous force system as it develops the highest damping force and sample 2 represents a yield stress value lesser than sample 4 which is displayed in Figure 5a.

However, checking the sedimentation and viscosity values, we find that sedimentation is high for sample 4 which is clearly shown in Figure 5b. The

Table 3. Measure of current and MF density

Current (A) / MF density	0.5	1	1.5	2	2.5
0.8	1.752	1.750	1.912	1.965	1.813
1	1.752	1.750	1.912	1.965	1.813
1.5	1.750	1.847	1.909	1.962	1.809
2	1.749	1.846	1.908	1.960	1.806
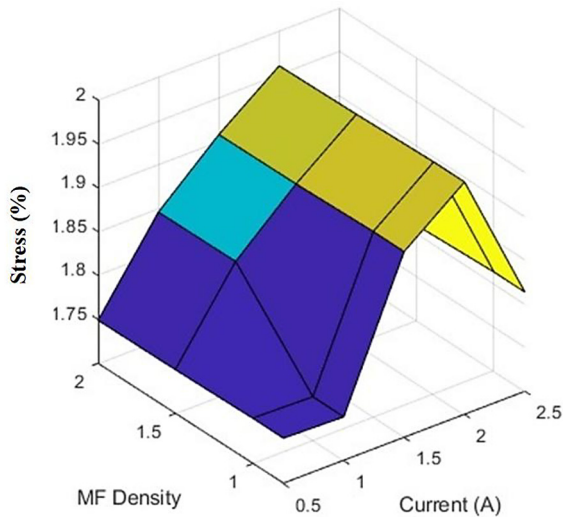
**Figure 4.** Stress and field density from MATLAB

The experiment documented the output damping force and displacement under various current levels as shown in Figure 6. The findings reveal that the output damping force has small changes with displacement. The frictional force decreases from -210 nN to -58 nN. The deviations from the curve can be ascribed to interference of the signal and low vibrations during the testing process. From the comparison of damping force-displacement curves at different currents, it was observed that as the excitation current increases, the damping force output of the damper also increases. Out of all the samples analyzed, the sample 2 exhibited the stable properties of the MR fluid indicate that it can be used for long term real use applications.

damped force and yield stress developed are slightly higher than that of sample 2. We took sample 2 as the best choice for the system from this comparison. It shows a higher sedimentation ratio and closer yield stress values to sample 4, Sample 2 has a damping force of 2130 N, the yield stress of 88 KPa and a sedimentation ratio of 0.89. The vibration excitation platform was set with a sinusoidal motion with amplitude of 12 mm and frequency of 1.5 Hz to assess the effect of different currents on the output damping force of the proposed damper. Moreover, the test system was weighted according to the weight of the damper in the system. A DC power supply was employed to control the values of the excitation currents that were applied to the damper.

Performance analysis of the proposed MR damper

The proposed optimized MR damper is design is visualize in 3D form in the ANSYS environment. Also, the parameter monitoring function and the damper controller is designed in the MATLAB environment**.** The velocity that lies among cylinder piston has raised the damping force, also the damping force is varied based on the fluid flow rate and stress. The measure of field intensity and flux density of the MR fluid and its 3D visualization with varying current is detailed in Figure 7 and Figure 8 without and with optimization using BGBM technique. Here, the reason for utilizing MR fluid in damper cylinder is for better flexibility range and wide
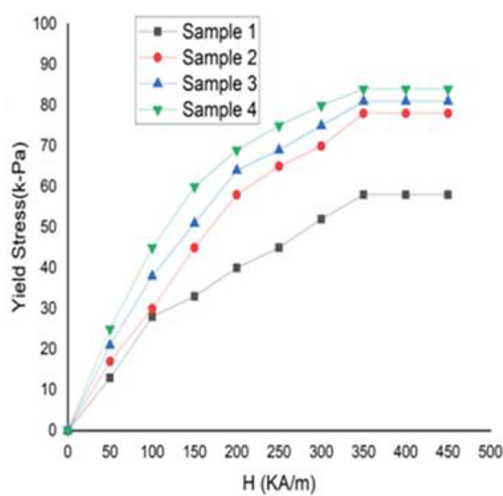
(a)
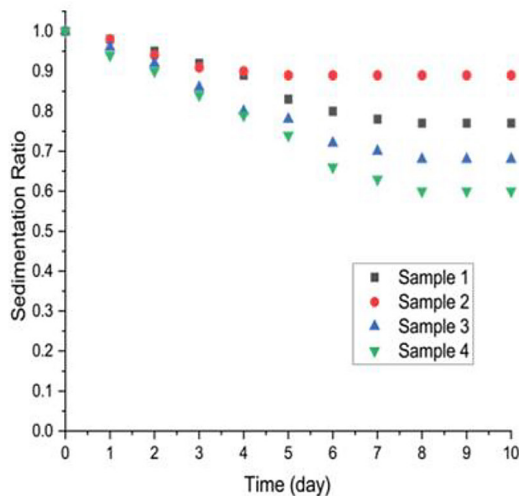
(b)

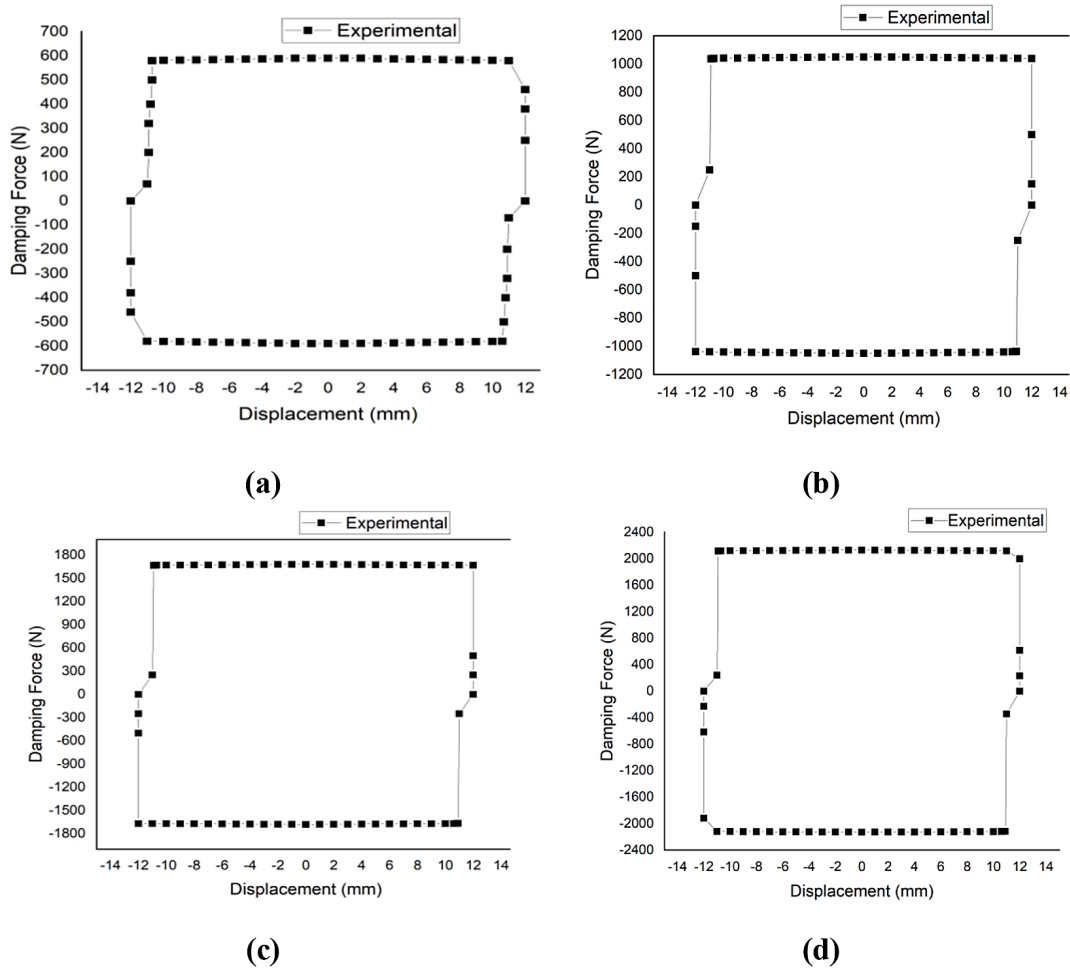**Figure 5.** Magnetic field vs yield stress (a), Time vs sedimentation ratio (b)

Figure 6. Experimental damping force under different currents: current of 0.2 A (a) current of 0.4 A (b), current of 0.1 A (c) current of 1.4 (d)

viscosity. Here, the flux density and magnetic field is calculated in two phases that is before and After validating the damper current without optimization, the tuning range's performance has been measured by valuing the damper's current after applying the optimization function.

In the damper's cylinder, the is created using a wounded copper coil in the piston's center location. Moreover, both the cylinder and piston of the damper are employed by permeable magnetic material. The flux line of magnitude has entered via both components (cylinder and piston) then the annular gap among them is noted.

The damping force was measured by varying the current from 0 A to 2 A, illustrated in Figure 9. Based on MR fluid dynamic viscosity rule, the control operations of damping force have been detailed as driving current and exterior magnetic field. Hence, considering the conventional dampers it has needed less energy to operate the function. Thus, it has recorded low energy consumption. In addition, the energy requirement is based on coil material and device size.

Here, the red dot line magnitude and distance measure of 0.5 A, the green dash line is the distance and magnitude measure for 1 A, the blue color dot line has denoted the performance of 1.5 A, and the orange color solid line has utilized to calculate the magnitude performance of 2 A current. The function of the designed damper is analyzed by some key metrics like Ground force, amplitude, and damper's energy. The amplitude-frequency of the damper was varied based on damping force and currently applied; from 38 Hz frequency, the force of the Damper is gradually decreased.

Comparative analysis of MR damper

To value the robustness of the presented intelligent BGBM damper, some of the conventional replicas were obtained that are optimized
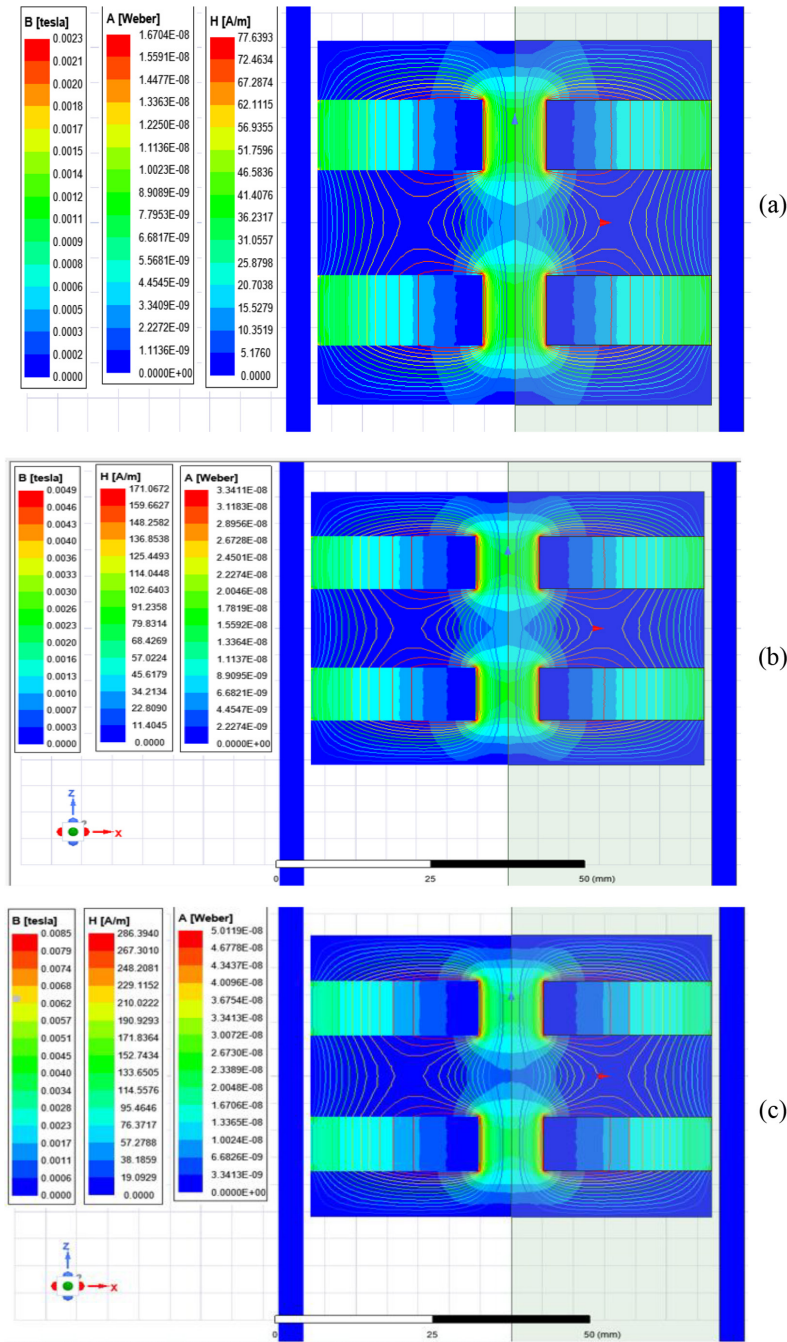
Figure 7. Damper current before optimization: 0.4A (a), 0.8A (b), 1.2A (c), 1.6A (d), 2A

damper MR damper with genetic and particle swarm algorithm [22], Genetic procedure with neural (GPN) [27], policy gradient neural network (PGNN) [27], model, sliding mode-hybrid adaptive control (SM-HAC) [27], Skyhook controller (SC) [28]. Table 4 issues the assessment results of Yield stress by comparing the various damping mechanism. In any application, the yield stress is greater than the yield strength; also the metrics stress is depended upon the elasticity range. In addition, Figure 10 has depicted the variation for all methods this is happened

because of, for 0.2 B the attained stress measure by Kirchhoff's- MR damper is 0 kPa, Heaviside MR damper is 0 kPa and the proposed BGBM damper also 0 kPa. For 0.4 B, the achieved stress measure by Kirchhoff's- MR damper is 20 kPa, Heaviside MR damper is 30 kPa and the proposed BGBM damper also 32 kPa.

For 0.6 B, the gained stress measure by Kirchhoff's- MR damper is 30 kPa, Heaviside MR damper is 58 kPa and the proposed BGBM damper also 60 kPa. For 0.8 B the obtained stress rate by Kirchhoff's- MR damper is 45 kPa,
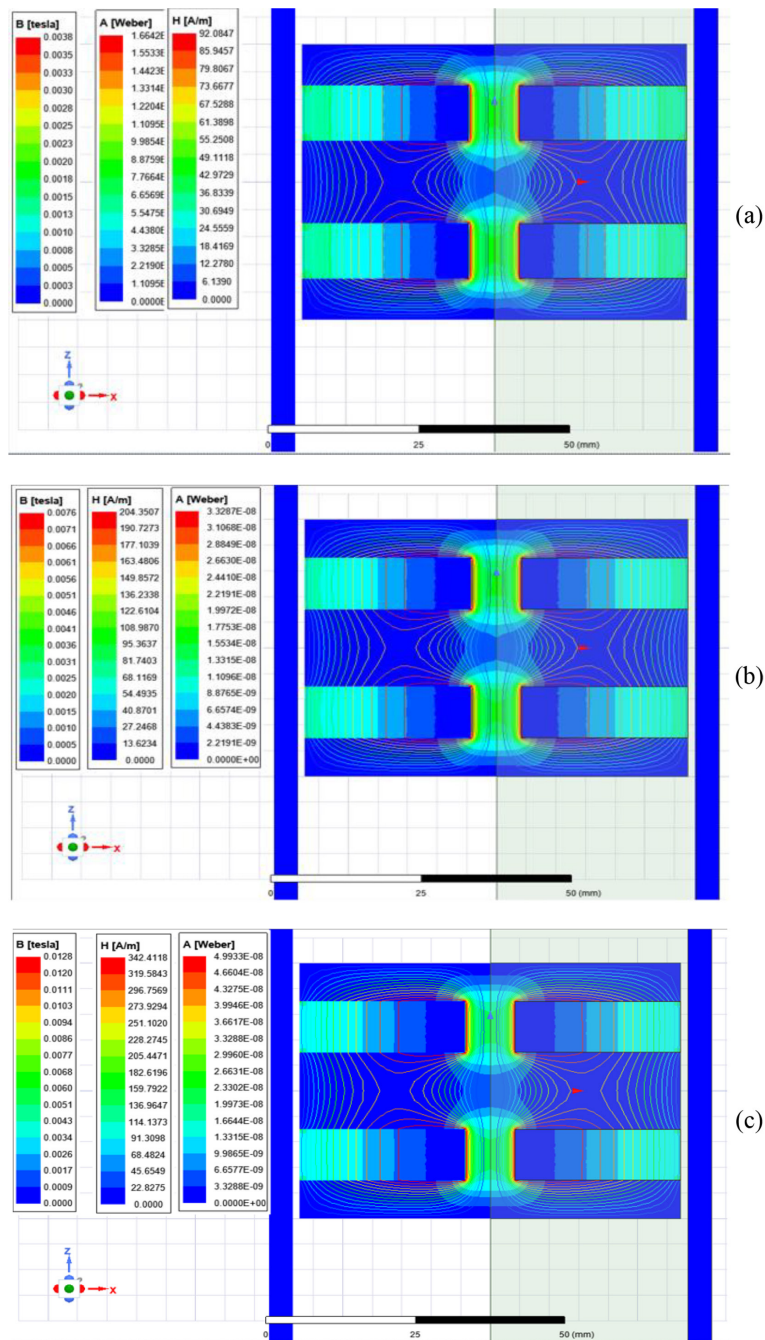
Figure 8. Damper current after optimization: 0.4A (a), 0.8A)b), 1.2A (c), 1.6A (d), 2A (e)

Heaviside MR damper is 80 kPa and the proposed BGBM damper also 90 kPa. For 1B, the earned stress score by Kirchhoff's- MR damper is 48 kPa, Heaviside MR damper is 80 Kpa and the proposed BGBM damper also 130 kPa. For 1.2 B, the attained stress measure by Kirchhoff's-MR damper is 50 kPa, Heaviside MR damper is 90 kPa and the proposed BGBM damper also 160 kPa. For 1.4 B, the attained stress measure by Kirchhoff's-MR damper is 50 kPa, Heaviside MR damper is 90 kPa and the proposed BGBM damper also 160 kPa.

Stroke, damping force and energy efficiency

The finest damping results have been obtained based on the dependent stroke characters and the stroke properties is lies among comfort and space of the suspension deflection. The comparative validation of stroke is projected in Figure 11.

The method GPN has reported the maximum stroke measure as 0.197 m, PGENN has reported the wide stroke measure as 0.194 m, SM-HAC has obtained the maximum stroke rate as 0.210 m, Sc has recorded the maximum stroke score as
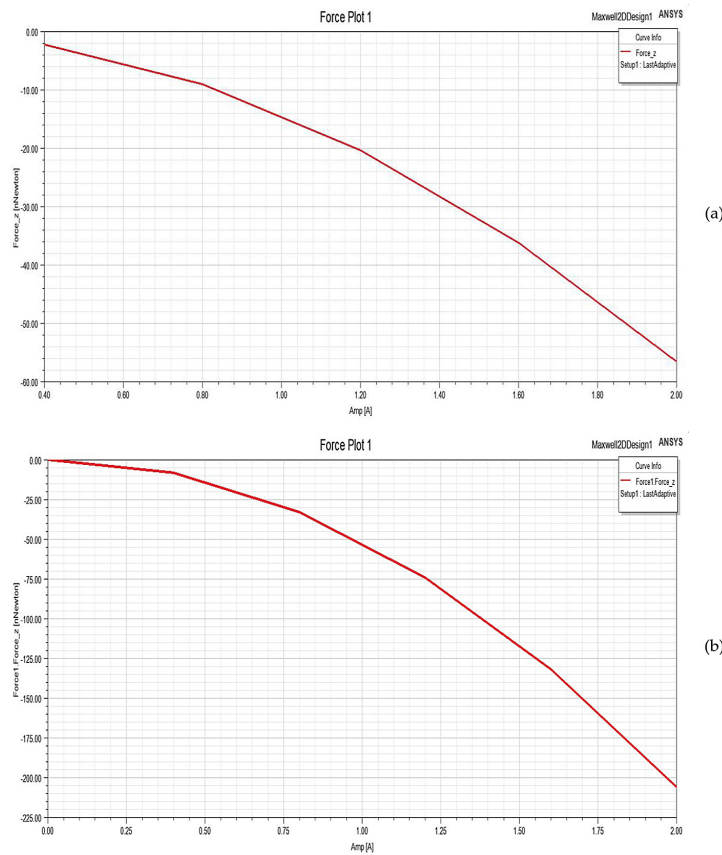
Figure 9. Friction force: before optimization (a), after optimization (b)

Table 4. Assessment of yield stress

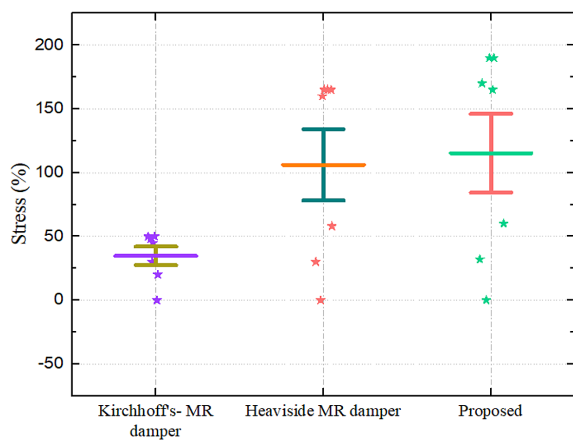| MF density B (Tesla)	Yield stress (kPa)		
	Kirchhoff's-MR damper [24]	Heaviside MR damper [22]	Proposed
0.2	0	0	0
0.4	20	30	32
0.6	30	58	60
0.8	45	70	90
1	48	80	130
1.2	50	90	160
1.4	50	90	160

Figure 10. Stress comparison

0.217 and the proposed BGBM damper has recorded the maximum stroke measure as 0.185 m. The assessment of damping force and energy is detailed in Figure 12.

The method GPN has earned 94.6% energy efficiency, 2.29 kN of damping force, PGENN has reported 95.9% energy efficiency, 2.28 kN damping force, SM-HAC has obtained the energy efficiency rate as 93.8%, damping force as 2.18 kN, consequently, the energy efficiency reported by the model SC is 90.6%, 2.18 kN damping force. Also, the proposed BGBM damper has recorded the energy efficiency rate as 96.7% and 2.4 kN damping force. Thus, comparing other approaches, the proposed
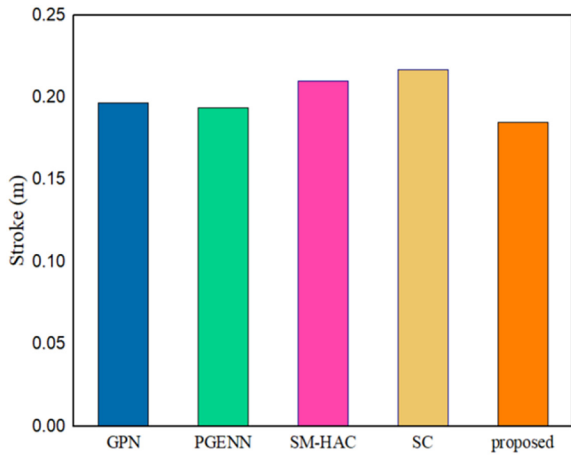
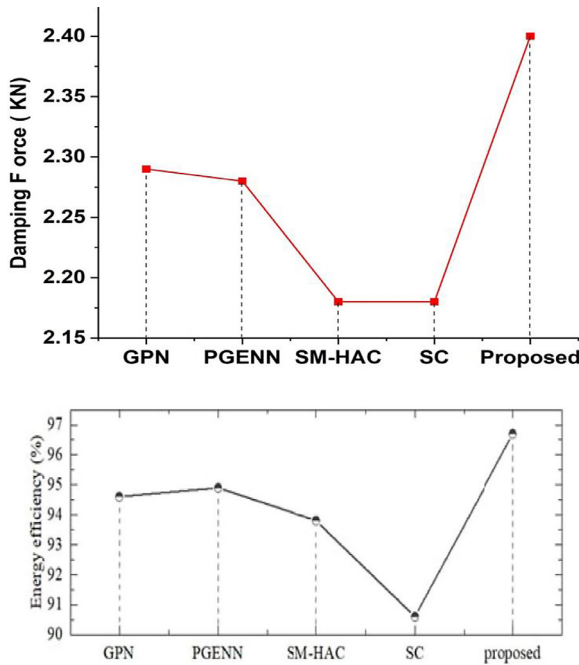**Figure 11.** Stroke comparative assessment

Figure 12. Damping force and energy efficiency assessment

BGBM has recorded the finest damping force and energy efficiency value. Thus the proposed BGBM model is highly proficient than other procedures.

Overall performance on proposed BGBM–MR fluid damper

From all the comparison assessments, it was verified that the designed BGBM-MR fluid damper has earned the finest performance in all metric cases. Also, the designed damper performance is checked with landing gear application. The overall assessment is detailed in Table 5.

By applying the landing gear application, some of the parameters is calculated such as ground force and amplitude range. Finally, the designed MR fluid damper based landing gear system is compared with other approaches and has recorded the finest outcomes.

CONCLUSIONS

In this research, the bat based gradient boost mechanism was used to design and optimize a Silicon and Iron based MR fluid damper. The performance of the proposed damper in a landing gear application was experimentally tested in two phases: with and without optimization. Damper based on the BGBM optimization provided better damping force, yield stress, as well as higher energy efficiency and represented good additional solution to a conventional system.

Experimental results indicated that Sample 2 was the most stable MR fluid formulation with damping force of 2130 N, yield stress of 88 kPa and sedimentation ratio of 0.89. Finally, the maximum damping force achieved by the final optimized damper was 2.4 kN, yield stress was 160 kPa, and stroke length 0.185 m. This, however, notched some slight discrepancies between theoretical and experimental results attributed to a number of real world factors. Deviation from simulation torque were greatly attributed to pre optimization friction, which was measured to be -210 nN, post optimization to -58 nN, thereby proving to represent dissipated internal energy. Frc is a function

Table 5. Overall performance of the proposed BGBM-MR fluid damper

Parameter	Stroke (max) [m]	Energy efficiency [%]	Damping force (max) [kN]
GPN	0.197	94.6	2.29
PGENN	0.194	94.9	2.28
SM-HAC	0.210	93.8	2.18
SC	0.217	90.6	2.18
Proposed	0.185	96.7	2.4

of MR fluid sedimentation, which was shown to have resulted in 5.1% variation in damping force due to nonuniform iron particle distribution. The impact of magnetic flux leakage and minor inconsistencies in field distribution introduced a 3.8% error in force measurements. At 1.5 Hz excitation, the response time lag affected the force output by 4.2%. Also, deviations up to 3.5% from theory were found to be due to structural tolerances and adjustments in damping gap thickness and coil dimensions. With these variations, BGBM optimized damper still preserve the advantages, 4% on the energy efficiency and 3% on the damping force, compared to the existing models.

Future research includes refining of predictive models, field testing of the influence of temperature dependent fluid behavior on the landing gear system, and long term durability testing of the system in production landing gear.

REFERENCES

1. Sam Paul P., Varadarajan A. S., and Mohanasundaram S., Effect of magnetorheological fluid on tool wear during hard turning with minimal fluid application. Archives of Civil and Mechanical Engineering 2015; 15(1): 124–132.

2. Yin, C., Huang, J., Quan, Q., Tang, D., Meng, L., Guo, F., Deng, Z., Technical progress in landing mechanisms for exploring small solar system bodies, Progress in Aerospace Sciences 2021; 122: 100697.

3. Mokhena, T.C., M. J. John., Cellulose nanomaterials: New generation materials for solving global issues, Cellulose 2020; 27(3): 1149–1194.

4. Gopinath B., Sathishkumar G.K., Karthik P., Charles M.M., Ashok K.G., Ibrahim M., Akheel M.M., A systematic study of the impact of additives on structural and mechanical properties of magnetorheological fluids, Materials Today: Proceedings 2021; 37: 1721–1728.

5. Kumar, J.S., Paul, P.S., Raghunathan, G., Alex, D.G., A review of challenges and solutions in the preparation and use of magnetorheological fluids, International Journal of Mechanical and Materials Engineering 2019; 14(1): 1–18.

6. Ali, b., Baghlani, A. Reliability assessment of MR fluid dampers in passive and semi-active seismic control of structures, Probabilistic Engineering Mechanics 2021; 63: 103114.

7. Kolekar, S., Venkatesh, K. Experimental investigation of damping effect in semi-active magnetorheological fluid sandwich beam under non-homogeneous magnetic field, Journal of Vibration Engineering & Technologies 2019; 7(2): 107–116.

8. Balaji P. S., Karthik Selva Kumar K. Applications of nonlinearity in passive vibration control: a review, Journal of Vibration Engineering & Technologies 2021; 9(2): 183–213.

9. Ankitha N., MRS Rupa Sri, Design and Analysis of shock absorber, recent trends in mechanical engineering. Springer, Singapore, 2021; 433–444.

10. Nguyen T.A.T., Chou, S.-Y. Maintenance strategy selection for improving cost-effectiveness of offshore wind systems, Energy Conversion and Management 2018; 157: 86–95.

11. Hashem A., Hossain M.M., Al Mamun M., Simarani K., Johan M.R. Nanomaterials based electrochemical nucleic acid biosensors for environmental monitoring: A review, Applied Surface Science Advances 2021; 4: 100064.

12. Rajnak M., Timko M., Kopcansky P., Paulovicova K., Kuchta J., Franko M., Cimbala R. Transformer oil-based magnetic nanofluid with high dielectric losses tested for cooling of a model transformer, IEEE Transactions on Dielectrics and Electrical Insulation 2019; 26(4): 1343–1349.

13. Banu J.R., Sharmila V.G., Ushani U., Amudha V., Kumar G. Impervious and influence in the liquid fuel production from municipal plastic waste through thermo-chemical biomass conversion technologies- A review, Science of the Total Environment 2020; 718: 137287.

14. Shuli W., Wang J., and Ou J. Method for improving the neural network model of the magnetorheological damper, Mechanical Systems and Signal Processing 2021; 149: 107316.

15. Bahiuddin I., Imaduddin F., Mazlan S.A., Ariff M.H., Mohmad K.B., Choi S.B., Accurate and fast estimation for field-dependent nonlinear damping force of meandering valve-based magnetorheological damper using extreme learning machine method, Sensors and Actuators A: Physical 2021; 318: 112479.

16. Da Silva J.A.I., Bueno D.D., De Abreu G.L., A strategy to suppress limit cycle oscillations in helicopter ground resonance including landing gear nonlinearities, Aerospace Science and Technology 2020; 105: 106011.

17. Dal-Seong Y., Kim G.-W., Choi S.-B. Response time of magnetorheological dampers to current inputs in a semi-active suspension system: Modeling, control and sensitivity analysis, Mechanical Systems and Signal Processing 2021; 146: 106999.

18. Mirzaei O.M., Jannesari H. Economic and environmental assessment of reusing electric vehicle lithium-ion batteries for load leveling in the residential, industrial and photovoltaic power plants sectors,

Renewable and Sustainable Energy Reviews 2019; 116: 109413.

19. Mohammad Z., Aalaie J. Application of shear thickening fluids in material development, Journal of Materials Research and Technology 2020; 9(5): 10411–10433.

20. Cruze D., Gladston H., Loganathan S., Dharmaraj T., Solomon S.M. Study on Magnatec oil-based MR fluid and its damping efficiency using MR damper with various annular gap configurations, Energy, Ecology and Environment 2021; 6: 44–54.

21. Azangbebil H., Djokoto S., Agelin-Chaab M. Experimental and numerical studies of a soft impact piezoelectric energy harvesting using an MR fluid, IEEE Sensors Journal 2020; 20(19): 11204–11211.

22. Asan G.A Muthalif, Khusyaie M., Razali M., Diyana Nordin N.H., Hamid S.B.A. Parametric estimation from empirical data using particle swarm optimization method for different magnetorheological damper models, IEEE Access 2021; 9: 72602–72613.

23. Munyaneza O., Sohn J.W. Design and geometric parameter optimization of hybrid magnetorheological fluid damper, Journal of Mechanical Science and Technology 2020; 34(7): 2953–2960.

24. Versaci M., Cutrupi A. Palumbo A. A magneto-thermo-static study of a magneto-rheological fluid damper: a finite element analysis, IEEE Transactions on Magnetics 2020; 57(1): 1–10.

25. Thiyagu M., Karunamoorthy L., Arunkumar N. Thermal and tool wear characterization of graphene oxide coated through magnetorheological fluids on cemented carbide tool inserts, Archives of Civil and Mechanical Engineering 2019; 19: 1043–1055.

26. Quoc Viet L., Jang D.-S., Hwang J.-H. Intelligent control based on a neural network for aircraft landing gear with a magnetorheological damper in different landing scenarios, Applied Sciences, 2020; 10(17): 5962.